Journal of
Mechanics of
Materials and Structures

EFFECTS OF LAYER STACKING ORDER ON THE V_{50} VELOCITY OF A TWO-LAYERED HYBRID ARMOR SYSTEM

Pankaj Kumar Porwal and Stuart Leigh Phoenix

Volume 3, Nº 4 April 2008

mathematical sciences publishers

JOURNAL OF MECHANICS OF MATERIALS AND STRUCTURES
Vol. 3, No. 4, 2008

EFFECTS OF LAYER STACKING ORDER ON THE V_{50} VELOCITY OF A TWO-LAYERED HYBRID ARMOR SYSTEM

PANKAJ KUMAR PORWAL AND STUART LEIGH PHOENIX

We develop a theoretical and computational model to investigate the ballistic response of a hybrid two-layered flexible armor system. In particular, we study the effects of stacking order of the two fibrous layers, which have distinctly different mechanical properties, on the V_{50} limit velocity. A system consisting of Kevlar and Spectra fabrics is studied in detail. For this system, previous experimental results of Cunniff show nearly a factor of two difference in the V_{50} velocities for the two possible stacking orders. The new model presented here extends our previous multilayer model by directly addressing interference effects between the two layers, treated here using length and tension compatibility along the radial direction away from the projectile. The primary task is to calculate strains in the individual layers in the presence of constraining interference that forces the nested layers to have a common impact cone shape different from what would be generated by the impact if the layers were allowed to deform freely. We show that this interference, together with relative areal densities of the layers, have a significant effect on the strain evolution in the layers, particularly near the edge of the projectile where failure initiates. As observed experimentally by Cunniff, our model predicts a large decrease in the V_{50} velocity of the hybrid armor system when Spectra is the strike layer. However, to achieve this reduction it is necessary to use a lowered normalization velocity in multilayered Spectra systems than the theoretical value obtained from basic fiber properties. Besides matching the experimental results of Cunniff, the model reveals many subtle transitions in the onset and effects of interference between the layers. Somewhat surprising and contrary to conventional wisdom is the observation that layer interference can sometimes be beneficial depending on the relative mechanical properties and areal densities of the two layers.

1. Introduction

The ballistic performance of a body armor system is usually measured in terms of the V_{50} velocity, the residual velocity when impacted above the V_{50} velocity, and the maximum deflection of the projectile in the armor system perpendicular to the plane of armor panel. There are two main focus areas in the development of low weight and high performance body armor systems: (a) development of materials with superior mechanical properties, and (b) design optimization of integrated system to efficiently translate these superior properties into ballistic performance. Fibrous body armors are constructed by stacking the woven or nonwoven layers of high performance fibers like aramid (Kevlar®), high molecular weight polyethylene (Spectra®), and until recently PBO (Zylon®). Others are still in development such as DuPont PIPD (M5®) and carbon nanotube based yarns. Modeling efforts to optimize the performance

Keywords: multilayered hybrid armor systems, stacking order, thermal effects, layer interference, V_{50} velocity, impact velocity versus residual velocity.

The authors acknowledge the support of the United States Air Force, contract no. USAF-5212-STI-SC-0013, monitored by Captain Todd J. Turner.

of armor systems have not kept pace with developments in new materials. Trial and error experimental investigation is very expensive and often ineffective due to a fundamental lack of understanding of the physics of the impact event and the mechanisms of yarn and layer failure, especially subtle interactions.

In this paper we analyze the two possible stacking orders of a hybrid two-layered system where, in one stacking order, the layers interfere with each other in the cone wave region. This interference results when the underlying layer attempts to form an incompatible cone shape with the top layer, when both layers are driven by a projectile velocity history during deformation. In the model, the momentum exchange between the interfering layers over time occurs primarily around the ring formed by the coincident cone wavefronts in the layers. The strain evolution in the layers is determined using length compatibility in the conical and in-plane deformation zones extending from the projectile edge to the tension wavefronts in the layers and tension compatibility from dynamic effects analogous to those seen in a belt traveling over a pulley at modest wrap angles. The case of a noninterfering arrangement of layers was treated in a previous work by the authors [Porwal and Phoenix 2005] and those results are also used in the comparison of the two stacking orders.

2. Literature survey

Earlier efforts to model the performance of a multilayered fibrous soft body armor system focused on either extrapolating results from a single layer system or assuming sequential failure through widely spaced layers where only one layer at a time engages the projectile, that is, a decoupled system [Roylance et al. 1973; Hearle et al. 1981; 1984; Taylor Jr. and Vinson 1989; Parga-Landa and Hernandez-Olivers 1995; Chocron-Benloulo et al. 1997; Cunniff 1999a; 1999b; 1999c; Billon and Robinson 2001; Zohdi 2002; Zohdi and Powell 2006]. Recently the authors have developed analytical models in which layers respond to the impact of a projectile in a coupled and synergistic manner, as they do in reality, but the layers are arranged in such a way that they form nested cones but without interference in the cone wave region or elsewhere [Phoenix and Porwal 2003; Porwal and Phoenix 2005].

It has been shown experimentally as well as by computer simulation models [Roylance et al. 1995] that constraining the transverse deflection of fabric layers, especially near the cone wavefront, significantly alters the strain distribution and hence the ballistic performance of the system. In a hybrid multilayered armor, the stacking order of the layers becomes critically important because it dictates the extent of interference between the layers in the cone of transverse deflection. Perhaps the best known demonstration of this effect is due to Cunniff [1992] who stacked Kevlar and Spectra layers in two possible arrangements and showed that the V_{50} velocity could be altered by about a factor of two.

3. Theoretical background for multilayered system behavior

The model developed here is based on the results from previous works by Phoenix and Porwal [2003] and Porwal and Phoenix [2005]. In those works, membranes with in-plane isotropic elastic properties are impacted normally by a flat-faced, right circular cylindrical (RCC) projectile with radius r_p and traveling at velocity V_p before the impact. Some of the results in those works will be the basis for the work here so we quote them without derivation. We note that all the results quoted below are not exact but are very accurate approximations, and should be understood as such.

We let Γ_{0i} be the areal density ratio of the ith layer relative to that of the projectile, that is,

$$\Gamma_{0i} = \frac{A_{\mathrm{d},i}}{A_{\mathrm{d,p}}} = \frac{m_{\mathrm{p}i}}{M_{\mathrm{p}}}, \tag{1}$$

where $A_{\mathrm{d},i}$ and $A_{\mathrm{d,p}}$ are the areal densities of the ith layer and the projectile, $m_{\mathrm{p}i} = A_{\mathrm{d},i}A_{\mathrm{p}}$ is the mass of the plug of the membrane material directly contacted by the projectile or right under it in the ith layer, and $M_{\mathrm{p}} = A_{\mathrm{d,p}}A_{\mathrm{p}}$ is the mass of the projectile. Here A_{p} is the projected area of the projectile onto the membrane plane, which is the same as the cross-sectional area of the RCC projectile impacting longitudinally. For a two-layered armor, the system areal density is

$$\tilde{\Gamma}_0 = \sum_{i=1}^{2} \Gamma_{0i}. \tag{2}$$

Upon impact of the projectile, there is a virtually instantaneous momentum transfer to the circular patches of the layers right under the projectile. Thus, the velocity of the projectile just after impact is

$$V_0 = \frac{V_{\mathrm{p}}}{1+\tilde{\Gamma}_0}. \tag{3}$$

Note that both layers respond instantaneously to the impact because there are negligible gaps between the layers. For the ith layer, the critical layer tensile strain just after impact occurs near the projectile edge, that is, at the projectile radius r_{p}. This strain is given by

$$\epsilon_{\mathrm{p}0i} = \left[\frac{V_0}{\sqrt{2}a_{0i}}\right]^{4/3}, \tag{4}$$

where a_{0i} is the tension wave velocity in the ith layer (approximately $\sqrt{E_i/2\rho_i}$), and E_i and ρ_i are the Young's modulus and density of the constituent yarns, respectively. The factor of 2 in the denominator comes from the added mass of crossing yarns that support no load in the direction of the wave propagation.

Two types of waves are formed just after the sudden local momentum transfer at time $t = 0$. The first type consists of radially growing tensile waves, and these are followed by much slower transverse waves in the form of growing cones with the projectile at their apexes. The projectile is decelerated by the membrane forces generated as the waves propagate in the layers. The velocity profile of the projectile is given by

$$V = \frac{V_{\mathrm{p}}}{1+\tilde{\Gamma}_0}\exp\left[-\frac{\sum_{i=1}^{2}\varphi_i\Gamma_{0i}\psi_i^2 + \sum_{i=1}^{2}(1-\varphi_i)\Gamma_{0i}\psi_{i,\mathrm{f}i}^2 - \tilde{\Gamma}_0}{1+\tilde{\Gamma}_0}\right], \tag{5}$$

where $\psi_i = r_{ci}/r_{\mathrm{p}}$ is the normalized cone wavefront position in the ith layer (where r_{ci} is the radius of the base of the conical deflection in that layer), $\psi_{i,\mathrm{f}i}$ is the normalized position of the cone wavefront in the ith layer when it fails, and

$$\varphi_i = \begin{cases} 0, & \text{for a failed layer,} \\ 1, & \text{for an intact layer.} \end{cases} \tag{6}$$

As the cone waves propagate, the changing strains in the layers at the projectile edge can be obtained by solving

$$\epsilon_{\mathrm{p}i} = \left(\frac{V}{a_{0i}\sqrt{2}}\right)^{4/3} {\psi_i}^{1/3} \left(\frac{\sqrt{\psi_i/\epsilon_{\mathrm{p}i}}(\psi_i - 1)}{\ln(1 + \sqrt{\psi_i/\epsilon_{\mathrm{p}i}}(\psi_i - 1))}\right)^{2/3}. \tag{7}$$

The material behind the tension wavefront flows toward the impact region. At the cone wavefront, the magnitude of this inflow velocity at time t is

$$\dot{u}_{ci} = \frac{a_{0i}\epsilon_{ci}r_{ci}}{r_{\mathrm{p}} + a_{0i}\,t}\left\{\ln\left(\frac{r_{ci}}{r_{\mathrm{p}} + a_{0i}\,t}\right) - 1\right\}, \tag{8}$$

which happens to be different for the two layers. Here $\epsilon_{ci} = \epsilon_{\mathrm{p}i}/\psi_i$ is the strain in the membrane at the cone wavefront. The cone wave generated by the transverse deformation of the membrane propagates into this inflowing material with velocity c_i in the material coordinate system, which in terms of the instantaneous projectile velocity V is given as

$$c_i = r_{\mathrm{p}}\frac{d\psi_i}{dt} = \text{const} \times a_{0i}\left(\frac{V}{a_{0i}\sqrt{2}}\right)^{2/3} = \text{const} \times {a_{0i}}^{1/3}\left(\frac{V}{\sqrt{2}}\right)^{2/3}. \tag{9}$$

The constant 'const' is typically a number slightly larger than 1 depending on the impact velocity, but in the subsequent calculations it suffices to take const $= 1$ (see [Phoenix and Porwal 2003]). The velocity of the cone wave in the ground coordinate system is $\tilde{c}_i = c_i + \dot{u}_{ci}$, which is somewhat less than c_i because $\dot{u}_{ci}$ is negative though much smaller. The tangential strain distribution in the membrane in terms of the strain in the membrane at the cone wavefront, ϵ_{ci}, can be written as

$$\epsilon_i \approx \frac{\epsilon_{ci}\,r_{ci}}{r}, \qquad r_{\mathrm{p}} \le r \le a_{0i}t + r_{\mathrm{p}}. \tag{10}$$

This can be integrated to estimate the change in length of the membrane material, Δl, in the radial direction due to the strain induced by the impact

$$\Delta l = \epsilon_{ci}r_{ci}\ln\left(\frac{a_{0i}t + r_{\mathrm{p}}}{r_{\mathrm{p}}}\right). \tag{11}$$

4. Model for interfering two-layered system

Let us consider a two-layered system deforming under a given projectile velocity history where both layers are in contact with each other under the projectile. Interference occurs when the transverse deflection of the top layer is hindered from forming its natural cone shape (when alone) by the underlying layer trying to form an incompatible cone shape. This is typically the case when the underlying layer has a lower Young's modulus and a higher material density and thus a lower tensile wave speed — though other factors are at play as well.

Figure 1 illustrates the situation in terms of the two nested layers. In particular, Figure 1(b) shows the case where the lower Kevlar layer exerts forces on the upper Spectra layer, causing the cone angle of Spectra to be larger than it would be if the layers were stacked in reverse order, as shown in Figure 1(a). Subscripts k and s denote the Kevlar and Spectra layers, respectively. An overbar is used for quantities corresponding to the interfering arrangement of the layers. In Figure 1, a_0 is the velocity of the tensile

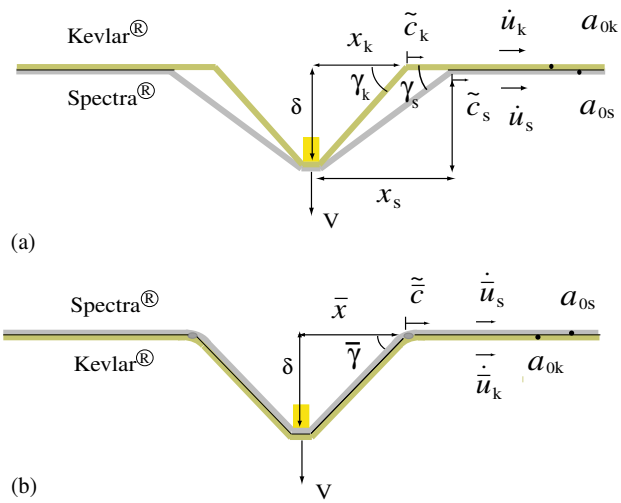

Figure 1. Effect of layer stacking order on the system response: (a) noninterfering arrangement (Kevlar–Spectra), versus (b) interfering arrangement (Spectra–Kevlar).

wave, $\tilde{c}$ is the velocity of the cone wavefront in the ground coordinate system, γ is the cone angle of transverse deflection with respect to ground, V is the instantaneous velocity of the projectile, and $\dot{u}$ is the material flow velocity, which turns out to be negative indicating that the material is flowing towards the impact region.

In the two-dimensional membrane model with constant projectile velocity, the portion of membrane that is right under the projectile moves with the projectile at the same velocity as the projectile, and with no velocity transverse to the projectile motion (that is, there is negligible slipping at the projectile edge). The material from the projectile edge to the cone wavefront forms a very mild curve [Phoenix and Porwal 2003] and can be approximated by a straight line to calculate its length. In the tensile wave region beyond the cone there is no significant interaction between the layers since there is no stitching or bonding. In the region of conical deformation, the material velocity is equal to that of the projectile. Thus, we can realistically assume that interaction forces between the layers only occur in the vicinity of the cone wavefront, that is, at the junction of the cone wave and tension wave (apart from the interaction between the plugs of layer material directly under the projectile).

For the interfering arrangement of the two layers, the basic assumption is that the cone wavefronts of both layers have the same velocity with respect to the ground coordinate system, and in fact the cone shapes are identical (Figure 1(b)). This, however, does not imply that the local strains along the cones and in the tension wave regions beyond the cones are the same in each layer; in fact, the tension wavefronts will be at different locations. In addition, each layer will be in tension out to its tensile wavefront, that is, there is no slack in either layer.

Based on compatibility of length implied by the identical cone shapes of the deformed layers, two equations can be written, which are

$$\sqrt{\delta^2+\bar{x}^2}+(x_{\mathrm{s}}-\bar{x})-\sqrt{\delta^2+x_{\mathrm{s}}^2}=(\bar{\epsilon}_{\mathrm{cs}}\bar{r}_{\mathrm{cs}}-\epsilon_{\mathrm{cs}}r_{\mathrm{cs}})\ln\left(\frac{r_{\mathrm{p}}+a_{0s}\,t}{r_{\mathrm{p}}}\right), \tag{12}$$

$$\sqrt{\delta^2+x_{\mathrm{k}}{}^2}+(\bar{x}-x_{\mathrm{k}})-\sqrt{\delta^2+\bar{x}^2}=(\epsilon_{\mathrm{ck}}r_{\mathrm{ck}}-\bar{\epsilon}_{\mathrm{ck}}\bar{r}_{\mathrm{ck}})\ln\left(\frac{r_{\mathrm{p}}+a_{0\mathrm{k}}\,t}{r_{\mathrm{p}}}\right), \tag{13}$$

where $\delta\int_0^t V(t)\,dt$ is the displacement of the projectile in the layers perpendicular to the plane of the armor panel. In the above equations $x_{\mathrm{s}}=\dot{c}_{\mathrm{s}}t$, $x_{\mathrm{k}}=\dot{c}_{\mathrm{k}}t$, and $\bar{x}=\tilde{\bar{c}}t$ are the bases of the approximately triangular shapes formed by the transverse deflection in the ground coordinate system, as shown in Figure 1. The radii of the bases of the cone wavefronts in the material coordinate system are

$$\bar{r}_{\mathrm{cs}}=r_{\mathrm{p}}+(\tilde{\bar{c}}-\dot{\bar{u}}_{\mathrm{cs}})t \quad \text{and} \quad \bar{r}_{\mathrm{ck}}=r_{\mathrm{p}}+(\tilde{\bar{c}}-\dot{\bar{u}}_{\mathrm{ck}})t, \tag{14}$$

for the Spectra and the Kevlar layers, respectively. These, however, are calculated incrementally because the velocities are not constant during the impact process. The left hand side of Equation (12), for the Spectra layer, is the extra length of material required to change its natural shape (as in Figure 1(a)) into the one that it is forced to form due to the interfering Kevlar back layer (as in Figure 1(b)). The right hand side of this equation represents the extra length of material generated by the increased strain in the layer, which is estimated using Equation (11). A similar interpretation can be applied to both sides of Equation (13). In Equation (14), the radially inward material flow velocities at the cone wavefronts of each layer are obtained by modifying Equation (8) as

$$\dot{\bar{u}}_{\mathrm{cs}}=\frac{a_{0\mathrm{s}}\bar{\epsilon}_{\mathrm{cs}}\bar{r}_{\mathrm{cs}}}{r_{\mathrm{p}}+a_{0\mathrm{s}}\,t}\left\{\ln\left(\frac{\bar{r}_{\mathrm{cs}}}{r_{\mathrm{p}}+a_{0\mathrm{s}}\,t}\right)-1\right\}, \tag{15}$$

$$\dot{\bar{u}}_{\mathrm{ck}}=\frac{a_{0\mathrm{k}}\bar{\epsilon}_{\mathrm{ck}}\bar{r}_{\mathrm{ck}}}{r_{\mathrm{p}}+a_{0\mathrm{k}}\,t}\left\{\ln\left(\frac{\bar{r}_{\mathrm{ck}}}{r_{\mathrm{p}}+a_{0\mathrm{k}}\,t}\right)-1\right\}. \tag{16}$$

A very helpful analogy for understanding the interaction forces between the two interfering cones is that of a pair of tensioned belts, one on top of the other and both running together over a pulley at modest wrap angle, as shown in Figure 2. We assume that the upper belt has a higher ratio of tension to linear density than the lower belt, which is in contact with the pulley. At a sufficiently high speed for the two

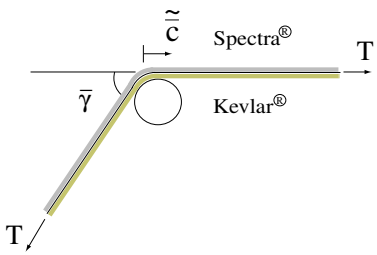

Figure 2. Belt-over-pulley analogy.

belts, yet maintaining the same total tension, the centrifugal forces of the belts around the pulley will become large enough for the lower belt to loose contact with the pulley despite the contact forces between the upper belt and lower belt. To connect this analogy to the problem of two interfering cones, the frame of reference is changed such that the pulley is traveling at the speed of the cone wavefront and the belts are stationary with respect to ground (see Appendix A for more details on the belt-over-pulley analogy). It should be noted that the individual tensions in the belts at the lift off threshold are not arbitrary but must be consistent with the length compatibility condition described earlier.

The combined tension in the two layers is

$$T = T_{\mathrm{s}} + T_{\mathrm{k}} = A_{\mathrm{s}} E_{\mathrm{s}}\, \bar{\epsilon}_{\mathrm{cs}} + A_{\mathrm{k}} E_{\mathrm{k}}\, \bar{\epsilon}_{\mathrm{ck}}, \tag{17}$$

where $A_{\mathrm{s}} = 2\pi(\bar{x} + r_{\mathrm{p}})h_{\mathrm{s}}$, $A_{\mathrm{k}} = 2\pi(\bar{x} + r_{\mathrm{p}})h_{\mathrm{k}}$, and h_{s} and h_{k} are the thicknesses of the Spectra and the Kevlar layers, respectively. From the belt-over-pulley analogy the tension in Equation (17) should also satisfy

$$T = \bar{\rho}\bar{A}\tilde{\bar{c}}^2, \tag{18}$$

where $\bar{\rho} = (A_{\mathrm{s}}\rho_{\mathrm{s}} + A_{\mathrm{k}}\rho_{\mathrm{k}})/\bar{A}$ and $\bar{A} = A_{\mathrm{s}} + A_{\mathrm{k}}$. Equations (17) and (18) can be combined to give

$$\bar{\rho}\bar{A}\tilde{\bar{c}}^2 = A_{\mathrm{s}} E_{\mathrm{s}}\, \bar{\epsilon}_{\mathrm{cs}} + A_{\mathrm{k}} E_{\mathrm{k}}\, \bar{\epsilon}_{\mathrm{ck}}. \tag{19}$$

For a given impact velocity we can solve Equations (12), (13), (15), (16), and (19) for the unknowns $\tilde{\bar{c}}$, $\dot{\bar{u}}_{\mathrm{cs}}$, $\dot{\bar{u}}_{\mathrm{ck}}$, $\bar{\epsilon}_{\mathrm{cs}}$, and $\bar{\epsilon}_{\mathrm{ck}}$. If the impact velocity is high enough then the critical strain in one of the layers will reach its failure value. In this case we continue the analysis further depending on which layer fails first.

Case 1: Strike layer fails first. If the Spectra strike layer fails first, at an instantaneous projectile velocity $V_{\mathrm{f,s}}$ and when the cone wavefront in the back layer is at $\psi_{\mathrm{k,fs}}$, then tension in the Spectra layer is relaxed, it is left behind, and only the back layer can actively decelerate the projectile. To determine whether the second layer is subsequently penetrated we revert to single layer behavior for the back layer. We must calculate a hypothetical initial impact velocity for a single layer system consisting of only the Kevlar layer, that will give the projectile velocity $V_{\mathrm{f,s}}$ with normalized position of the cone wave $\psi_{\mathrm{k,fs}}$:

$$V_{\mathrm{p,fs}} = V_{\mathrm{f,k}}(1 + \Gamma_0) \exp\left\{ \frac{\Gamma_0}{1 + \Gamma_0} (\psi_{\mathrm{k,fs}}^2 - 1) \right\}. \tag{20}$$

The Kevlar layer of the hybrid system is assumed to be penetrated if $V_{\mathrm{p,fs}}$ is higher than its ballistic limit when impacted alone; otherwise the projectile is stopped.

Case 2: Back layer fails first. If the Kevlar back layer fails first, that is, a plug of material in front of the projectile is severed and a hole is formed, then this penetrated layer will still be pushed along by the Spectra layer. The Kevlar layer will tend to recover its tension some distance away from the projectile edge due to the hoop stresses in the cone wave region of the punctured layer. However, the tension originally supported by the Kevlar back layer in the vicinity of the projectile edge must now be carried by the Spectra layer, thus locally increasing its strain. This strain can be calculated as

$$\bar{\epsilon}_{\mathrm{ps,fk}} = \frac{A_{\mathrm{s}} E_{\mathrm{s}} \bar{\epsilon}_{\mathrm{ps}} + A_{\mathrm{k}} E_{\mathrm{k}} \bar{\epsilon}_{\mathrm{pk}}}{A_{\mathrm{s}} E_{\mathrm{s}}}, \tag{21}$$

and if it is higher than the failure strain of the Spectra layer then this layer is also penetrated and the armor is defeated.

The smallest impact velocity at which both layers eventually fail, irrespective of which one fails first, is called the V_{50} velocity of the system.

5. Results and discussion

The physical and mechanical properties used for calculations are representative of the Kevlar and Spectra fibers as given in Table 1. Note that for these calculations the areal densities Γ_{0i} are replaced by $\theta^2\Gamma_{0i}$ to account for the uncertainty in the impact area. Here $\theta = 1.3$ is used (this value was found applicable to a wide range of data and material types in [Phoenix and Porwal 2003]) to reflect an increase in the effective contact area relative to the radius of the RCC projectile nose. We also show some results from [Porwal and Phoenix 2005] for a noninterfering stacking of the layers. Readers are referred to this paper for more details.

Figure 3 plots the strain evolution in the two layers of the hybrid system for both interfering and noninterfering arrangements of the layers, at impact velocity $V_p = 140$ m/s. The strains in each of the layers near the projectile edge first increase up to a maximum and then decrease as the cone wavefronts in both the layers propagate. This is similar to the case of a single layer or noninterfering arrangement of layers. Interference between the layers as well as their relative areal densities significantly alters the strains in both the Kevlar and Spectra layers. Interference decreases the strain in the Kevlar layer, in general, because of the widening cone base relative to its natural noninterfering shape. Conversely, the strain in the Spectra layer increases because of the smaller cone base radius formed in the interfering arrangement. In the case of an armor system consisting of predominantly Spectra, for example, $A_{d,k} = 0.01\,\text{kg/m}^2$ and $A_{d,s} = 0.46\,\text{kg/m}^2$, the strain in the Kevlar at the projectile edge drops significantly without affecting the strain in the Spectra layer because Spectra can easily push the thin layer of Kevlar to widen its cone shape. On the other hand, for the system consisting of predominantly Kevlar , the Kevlar strain remains unchanged and the strain in Spectra increases significantly. However, when $A_{d,k} = 0.29\,\text{kg/m}^2$ and $A_{d,s} = 0.18\,\text{kg/m}^2$ then strains in the Spectra and Kevlar are both altered significantly.

Figure 4 shows the effect of stacking order of the layers on the V_{50} limit velocity as well as on residual velocity when impacted above the V_{50} velocity for the specific combination of Kevlar areal density, $A_{d,k} = 0.29\ \text{kg/m}^2$, and Spectra areal density, $A_{d,s} = 0.18\,\text{kg/m}^2$. For the interfering arrangement of layers, the combined effects of strength loss due to thermal softening and an increase in the strain due to interference for the Spectra layer reduces the V_{50} velocity from 216 m/s (with $\epsilon_{s,fail} = 0.035$), for the noninterfering arrangement, to 156 m/s (with $\epsilon_{s,fail} = 0.021$ due to thermal softening). Our theory confirms the experimental observation of Cunniff [1992], however, his results exhibited a greater

Projectile		**Fibers**		
		Property	Spectra	Kevlar
Radius	2.76 mm	Stiffness, E	120 GPa	73 GPa
Weight	16 grain	Density, ρ	970 kg/m^3	1440 kg/m^3

Table 1. Right circular cylindrical (RCC) projectile, with length to diameter ratio 1, and fiber properties used for calculations.

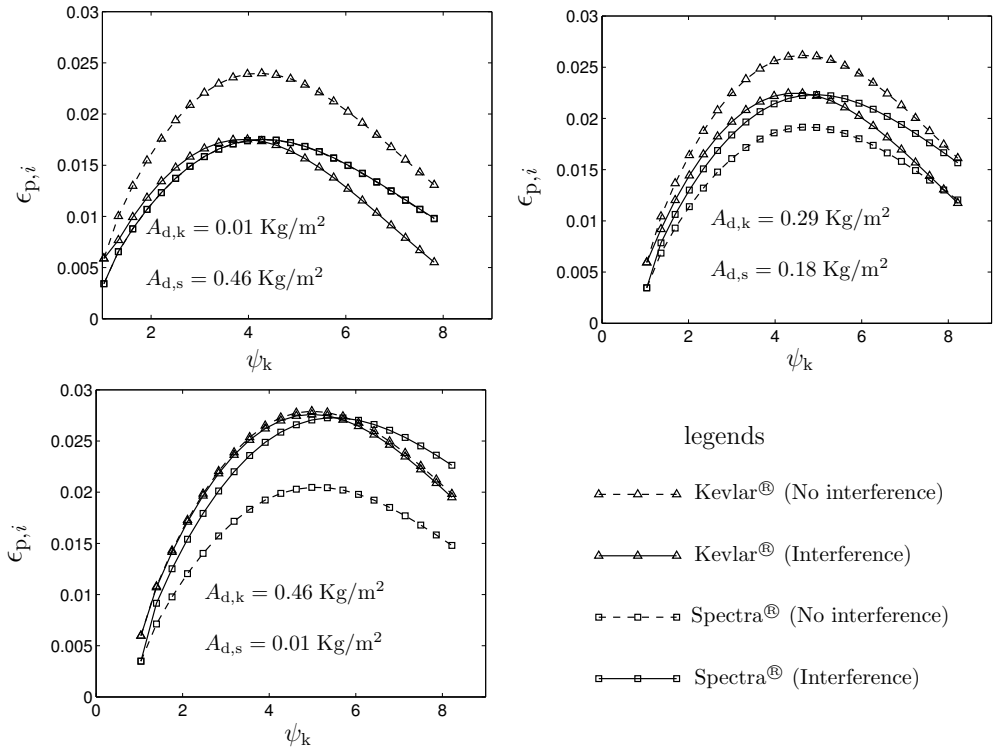

Figure 3. Strains in the layers around the projectile tip versus normalized cone wavefront for both interfering and noninterfering arrangements under impact velocity $V_{\mathrm{p}} =$ 140 m/s. The x-axis coordinate, ψ_k, is the wavefront position of the Kevlar layer when in the noninterfering arrangement. In the first figure the strains for interfering and noninterfering arrangement coincide for Spectra layer.

difference in V_{50} performance for the two possible arrangements, that is, 269 m/s versus 114 m/s. Note that if softening does not occur then the difference in performance for the two possible arrangements is only slight. Thus, while we can create a scenario to match the results of [Cunniff 1992] it can only be done by invoking severe thermal softening of the thin Spectra layer.

We have also investigated the V_{50} velocity for other areal density combinations of Spectra and Kevlar layers as shown in Figure 5, which plots the V_{50} velocity versus the areal density of Kevlar layer. In the comparison, the total areal density of the system is kept constant, that is, $A_{\mathrm{d}} = A_{\mathrm{d,k}} + A_{\mathrm{d,s}} = 0.47$ kg/m^2. The family of curves corresponds to different failure strains for the Spectra . Also shown are plots for the individual Kevlar and Spectra layers, when impacted alone, for the failure strains shown in the figure. Obviously, the effects of interference are modest unless one also invokes thermal softening effects in terms of reduced failure strain of the Spectra when it is the strike layer. When the failure strain is held fixed for both arrangements, the largest effect of interference compared to no interference is seen at $A_{\mathrm{d,k}} \approx 0.16$ for $\epsilon_{\mathrm{s,fail}} = 0.045$ and $\epsilon_{\mathrm{k,fail}} = 0.036$. In this case the V_{50} velocities for the interfering and noninterfering arrangement of the layers are 224 versus 289 m/s. Also, for a fixed $\mathrm{A_{d,k}}$ ($\mathrm{A_{d,k}} = 0.20$, for

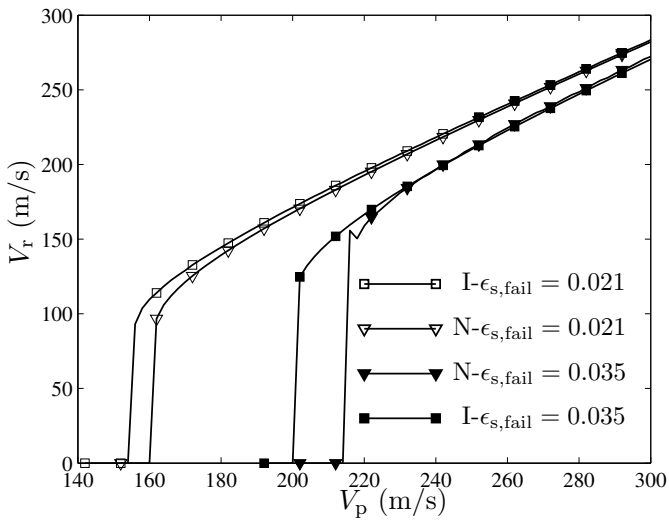

Figure 4. V_r versus V_p curves for a two-layered hybrid system consisting of Kevlar ($A_{d,k} = 0.29$ kg/m^2) and Spectra ($A_{d,k} = 0.18$ kg/m^2) layers. The failure strain of the Kevlar is $\epsilon_{k,fail} = 0.036$ for all cases. In legends I and N correspond to interfering and noninterfering arrangements of the layers, respectively.

example) and different failure strains, there are transitions between the situations in which interference degrades performance versus enhances performance, though only modestly. At these transitions, the sequential order in which the layers fail often reverses. The locations of these transitions depend on the relative failure strains of the layers. This is so because the ability a layer to withstand the load without penetration, for a given projectile impact velocity, depends not only on its own failure strain but also on contribution of other layers in decelerating the projectile before they are penetrated.

6. Conclusions

This paper is the third in the series of papers we have written to model the performance of multilayered fibrous soft body armor systems analytically. Here, we make an attempt to explain the experimental results of Cunniff [1992] using typical mechanical properties for the Kevlar and Spectra layers. The only fitting parameter used in the calculations is $\theta = 1.3$ to reflect an expanded plug of fabric in the initial momentum exchange.

Appendix A: Belt-over-pulley analogy

Figure 6 shows a tensioned belt traveling over a pulley at a speed c. In the case of a membrane this would be a section of the membrane traveling over a ring in the plane of the membrane. Let us consider a small element BO′B′ of this belt that subtends an angle $d\phi$ such that $\sin d\phi \approx d\phi$ at the center of the pulley. This element experiences three different forces. The first is the tensile force from the belt, which is approximately the same at each end of the element. The resultant of these two tensile forces acts in

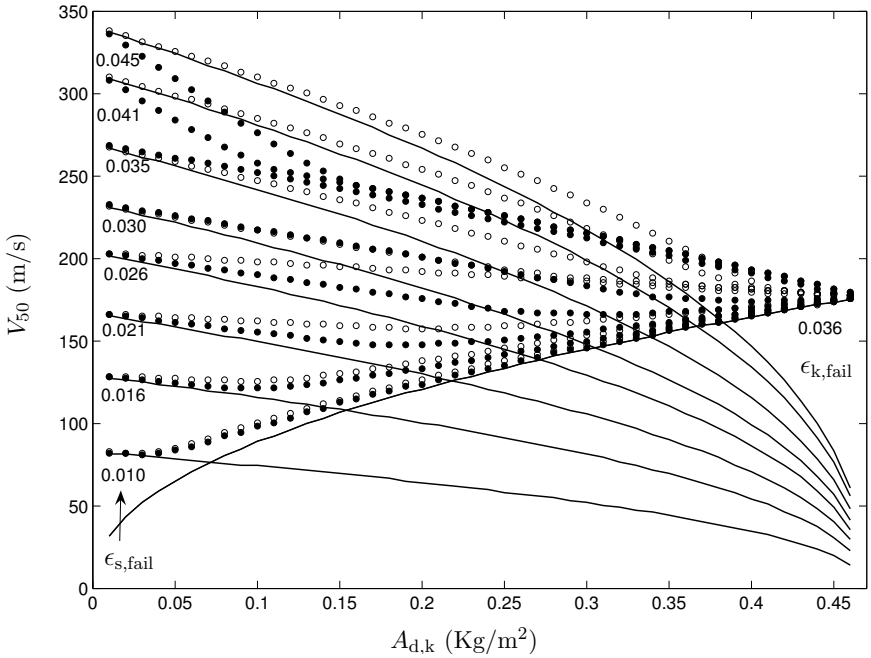

Figure 5. V_{50} velocity of the hybrid (Kevlar and Spectra) armor system versus areal density of the Kevlar layer, $A_{\mathrm{d,k}}$, for various failure strain combinations for the constituent layers. The total system areal density is $A_{\mathrm{d}} = A_{\mathrm{d,k}} + A_{\mathrm{d,s}} = 0.47$ kg/m^2. The solid and hollow circular markers correspond to interfering and noninterfering arrangements of the layers, respectively. The solid lines correspond to the V_{50} velocity of the individual Kevlar and Spectra layers.

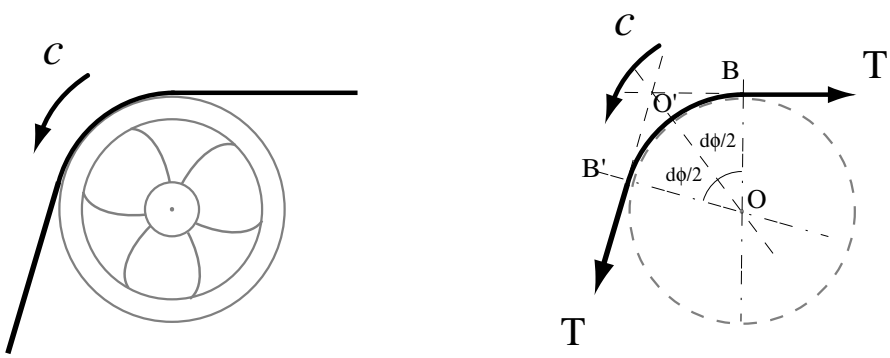

Figure 6. Illustration of the belt-over-pulley analogy.

the O′O direction, which bisects the angle subtended by the element, and has a magnitude

$$T_{O'O} = 2T \sin d\phi/2 \approx T d\phi = A E_f \epsilon_c d\phi, \tag{A.1}$$

where A is the cross-sectional area of the belt, E_f is the Young's modulus of the belt, and ϵ_c is the longitudinal tensile strain in the belt at the point of contact with the pulley, that is, point O′. The second force is the centrifugal force that the element experiences because of its motion on a circular path at speed c. The centrifugal force acts in the OO′ direction, and its magnitude is given by $F_c = \rho A c^2 d\phi$, where ρ is the density of the belt material. A contact force between the belt element and the pulley is the third force that acts on the element. For the purpose of our problem we can assume the contact between the belt and the pulley to be frictionless, as explained later. Under this assumption the contact force will act in a direction normal to the surface of the pulley at the contact point, that is, along OO′ direction. The magnitude of the normal contact force, N, can be obtained by considering the linear momentum balance for the element in the OO′ direction, which gives

$$N = A E_f \epsilon_c d\phi - \rho A c^2 d\phi. \tag{A.2}$$

The component of the tensile force along O′O direction is independent of the speed c, whereas the centrifugal force is proportional to the square of this speed. Thus, the magnitude of the normal contact force decreases with c. There exists a speed at which the normal contact force becomes zero. At this speed the presence of the pulley is immaterial and the situation is equivalent to the cone wavefront in the ballistic impact problem. Furthermore, at this instance of zero normal contact force, the frictional forces will be zero for both the frictional and frictionless contact between the pulley and the belt.

Thus from Equation (A.2), with $N = 0$, we have

$$A E_f \epsilon_c = \rho A c^2, \tag{A.3}$$

or

$$\epsilon_c = \frac{c^2 \rho}{E_f} = \left(\frac{c}{a_0}\right)^2 = \alpha^2, \tag{A.4}$$

where $a_0 = \sqrt{E_f/\rho}$ is the tensile wave velocity in the belt and $\alpha = c/a_0$. Equation (A.4) gives the relationship between the strain in the belt at the cone wavefront, the cone wave velocity, and the tension wave velocity in the impact problem as obtained by Phoenix and Porwal [2003]. One thing to note is that in the impact problem, the velocity c is not known exactly and hence the strain calculated using Equation (A.4) will be an approximation to the actual strain.

Of interest to the two-layered hybrid armor system is the case of two stacked belts passing over the pulley. In this case the top belt can press the bottom belt against the pulley even when the bottom belt has insufficient tension to maintain contact when by itself. This is the situation that arises in the case of interference. In this case, when the speed is high enough for the contact force between the bottom belt and pulley to vanish, Equation (A.3) can be modified to give

$$A_s E_s \bar{\epsilon}_{cs} + A_k E_k \bar{\epsilon}_{ck} = \bar{\rho} \bar{A} \tilde{\bar{c}}^2, \tag{A.5}$$

where the left hand side is the component of tensile forces in the pair of stacked belt elements along the O′O direction, and the right hand side is the centrifugal force experienced by the same. The symbols have the usual meanings.

References

[Billon and Robinson 2001] H. H. Billon and D. J. Robinson, "Model for the ballistic impact of fabric armour", *International Journal of Impact Engineering* **25**:4 (2001), 411–422.

[Chocron-Benloulo et al. 1997] I. S. Chocron-Benloulo, J. Rodriguez, and V. Sanches-Gelvez, "A simple analytical model to simulate textile fabric ballistic impact behaviour", *Textile Research Journal* **67**:7 (1997), 520–528.

[Cunniff 1992] P. M. Cunniff, "An analysis of the system effects in woven fabrics under ballistic impact", *Textile Research Journal* **62**:9 (1992), 495–509.

[Cunniff 1999a] P. M. Cunniff, "Decoupled response of textile body armor", pp. 814–821 in *Proceedings of 18th International Symposiam of Ballistics*, 1999.

[Cunniff 1999b] P. M. Cunniff, "Dimensional parameters for optimization of textile-based body armor systems", pp. 1303–1310 in *Proceedings of 18th International Symposiam of Ballistics*, 1999.

[Cunniff 1999c] P. M. Cunniff, "Vs-Vr relationships in textile system impact", pp. 814–822 in *Proceedings of 18th International Symposiam of Ballistics*, 1999.

[Hearle et al. 1981] J. W. S. Hearle, C. M. Leech, A. Adeyefa, and C. R. Cork, "Ballistic impact resistance of multi-layer textile fabrics. Final Technical Report", Technical report AD-A128064, University of Manchester Institute of Science and Technology, 1981.

[Hearle et al. 1984] J. W. S. Hearle, C. M. Leech, and C. R. Cork, "Textile ballistic performance (Data Base). Final Technical Report", Technical report AD-A143249, European Research Office, United States Army, 1984.

[Parga-Landa and Hernandez-Olivers 1995] B. Parga-Landa and F. Hernandez-Olivers, "An analytical model to predict impact behaviour of soft body armors", *International Journal of Impact Engineering* **16**:3 (1995), 455–466.

[Phoenix and Porwal 2003] S. L. Phoenix and P. K. Porwal, "A new membrane model for the ballistic impact response and V_{50} performance of multi-ply fibrous system", *International Journal of Solids and Structures* **40** (2003), 6723–6765.

[Porwal and Phoenix 2005] P. K. Porwal and S. L. Phoenix, "Modeling of system effects in ballistic impact into multi-layered fibrous structures for soft body armors", *International Journal of Fracture* **135**:1-4 (2005), 219–251.

[Roylance et al. 1973] D. Roylance, A. Wilde, and G. Tocci, "Ballistic impact of textile structures", *Textile Research Journal* **43**:1 (1973), 34–41.

[Roylance et al. 1995] D. Roylance, P. Hammas, J. Ting, H. Chi, and B. Scott, "Numerical modeling of fabric impact. high strain rate effects on polymer, metal and ceramic matrix composite and other advanced materials", *ASME* **48** (1995), 155–160.

[Taylor Jr. and Vinson 1989] W. J. Taylor Jr. and J. R. Vinson, "Modeling ballistic impact into flexible materials", *American Institute of Aeronautics and Astronautics Journal* **28**:12 (1989), 2098–2103.

[Zohdi 2002] T. I. Zohdi, "Modeling and simulation of progressive penetration of multilayered ballistic fabric shielding", *Computational Mechanics* **29** (2002), 61–67.

[Zohdi and Powell 2006] T. I. Zohdi and D. Powell, "Multiscale construction and large-scale simulation of structural fabric undergoing ballistic impact", *Computer Methods in Applied Mechanics and Engineering* **195**:1-3 (2006), 94–109.

Received 28 Mar 2007. Revised 31 Jul 2007. Accepted 1 Aug 2007.

PANKAJ KUMAR PORWAL: pporwal@iitb.ac.in
227 Department of Civil Engineering, Indian Institute of Technology, Powai, Mumbai 400076, India
http://www.civil.iitb.ac.in/~pporwal

STUART LEIGH PHOENIX: slp6@cornell.edu
Department of Theoretical and Applied Mechanics, 321 Thurston Hall, Cornell University, Ithaca, NY 14853, United States
http://www.tam.cornell.edu/Phoenix1.html